ISSN: 2664-9640

Structural subsidence characteristics and numerical simulation in the south of Ordos Basin-Taking Well Xuntan1 as a example

Baize Kai [1], Dengfa He [1] and Lei Zhou [2]

[1] School of Energy Resources, China University of Geosciences, Beijing 100083, China;

[2] The 8th Team of Daqing Logging & Testing Services Company, Daqing, 163000, China

Abstract

In this paper, taking the Well Xuntan-1 of the Weibei uplift in the south of the basin as an example, through the determination of the parameters such as the denudation thickness, the relationship between the porosity of different lithology and the depth, and the average density, etc., the structural subsidence of this well from the Middle Cambrian to the present in the south of the basin was accurately described.Based on the curve of structural subsidence, the period of structural subsidence was divided into three stages. At the same time, combined with the analysis of the tectonic background of the surrounding area , based on basin subsidence models caused by thermal cooling and foreland flexure, the structural subsidence of Well Xuntan-1 was studied. Through simulation, the southern part of Ordos basin has experienced three stages of rapid subsidence since the Middle Cambrian. The first stage was the Middle Cambrian, and the subsidence mechanism was thermal cooling subsidence. The second stage was from Late Permian to Middle Triassic. The subsidence mechanism was the thermal cooling subsidence caused by volcanism changing the geothermal gradient of the basin. The third stage of rapid subsidence wa early Cretaceous, and the subsidence mechanism was the flexural subsidence caused by the intracontinental orogeny in the southern Qinling Mountains and the thermal cooling subsidence together.

Keywords

Structural subsidence; Well Xuntan-1; Structural subsidence genesis numerical simulation; Composite structural subsidence genesis.

1. Introduction

As an important accumulation area of oil and gas, the formation and evolution of basins are often closely related to the tectonic movement of the mountains around the basin. According to the main methods of prototype basin analysis [1], the analysis of prototype basins is mainly conducted from three aspects: Time, Space, and Material. The study of basin subsidence history is an important part of basin space research. It is possible to describe the cause of the formation of the basin to a certain extent.

The Ordos Basin is located on the western margin of the North China Plate. It is a multi-cycle craton basin based on the basis of the Proterozoic basement. Its formation and evolution are affected by the peripheral orogenic movement, and multi-phase tectonic movements are superimposed on each other to finally form the present basin pattern. The research on tectonic subsidence in the basin was mainly concentrated in the Yishan slope area on the western margin of the basin, the northern section of the western margin and the Upper Paleozoic in the middle of the basin[2-4]. At present, the research on the characteristics of tectonic subsidence in the southern part of the basin lacks bottom-up and systematic research. As a key exploratory well on the Weibei Uplift, Well Xuntan 1 has comprehensive stratification data, logging data, and geochemical data. The study on the structural subsidence characteristics of Well Xuntan 1

ISSN: 2664-9640

is conducive to exploring the Subsidence mechanism in the southern part of the basin under the combined effect of multiple factors.

In this study, the Xuntan 1 well on the southern margin of the basin was carefully studied, combined with the research results of denudation, paleo-water depth, and the relationship between porosity and depth, etc., and the back stripping method was used to analyze the structural subsidence characteristics of the Xuntan 1 well. At the same time, combined with the thermal depression model and the foreland basin deflection model, a forward simulation of the structural subsidence curve of Well Xuntan 1 was carried out, and the cause of structural subsidence under the combined action of various factors in Well Xuntan 1 was discussed.

2. Regional geological background of the study area

2.1. Tectonic position of southern margin of Ordos basin

Ordos Basin is located in the northwest of North China Plate, surrounded by Qinling orogenic belt in the south, Liupan Mountain in the southwest, Helan Mountain in the northwest, Yin Mountain in the north and Lvliang Mountain in the east. This basin is a typical multi-cycle superimposed basin (Fig.1). The study area is located in the south of the basin, mainly composed of Weibei uplift, western margin thrust belt, Tianhuan depression, Yishan slope, Weihe basin and Qinling fold belt. The formation and evolution of the southern Ordos Basin are affected by the closure of Qinling-Qilian trough in the southern margin, and are also closely related to the formation of Qinling fold orogenic belt.

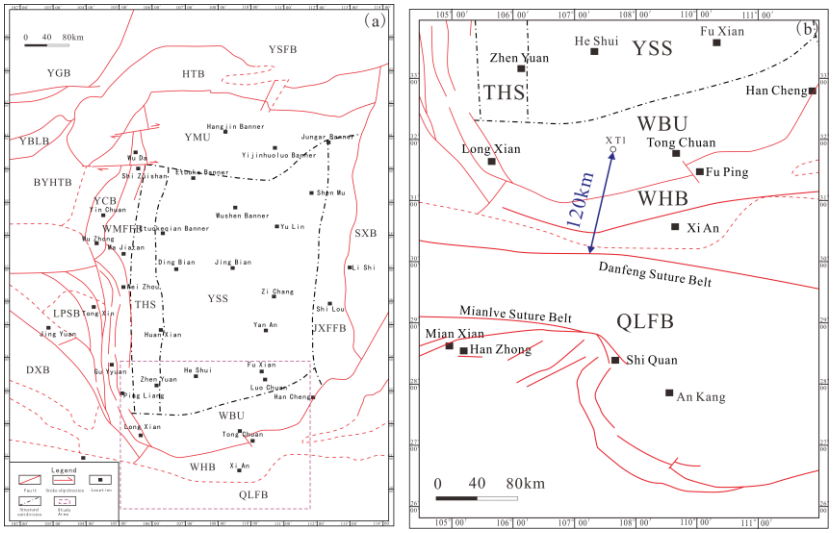

Fig.1 Location map of The Southern Ordos Basin

2.2. Main stratigraphic systems in the southern margin of the basin

The basement of the southern margin of the basin is widely developed, revealing Archean and Paleoproterozoic strata. The lithology is biotite plagioclase gneiss, dolomite schist and siliceous strip crystalline limestone. The main lithology of Cambrian and Ordovician is limestone, sandy and carbonaceous slate. The Caledonian movement which began in the late Ordovician caused the uplift and erosion of North China. The basin sedimentary discontinuity was more than 100 million years, and the late Ordovician, Silurian, Devonian and early-middle Carboniferous deposits were generally missing. The Late Carboniferous strata containx multi-layer coal seams, and volcanic rocks can also be seen. The overlying Permian strata is a set of marine-continental transitional facies deposits, and is mainly dominated by sandstone, siltstone and mudstone interbeds, with local coal seam lines. The lithology of Jurassic and Cretaceous is mainly dominated by sandstone, conglomerate and glutenite. The Cenozoic extension-convergence cycle includes two periods of large regional unconformity (Paleocene-Oligocene bottom,

ISSN: 2664-9640

Miocene bottom). Oligocene deposits are few, and the Quaternary is a thick glutenite layer,and a small amount of this formation was missing (Fig.2).

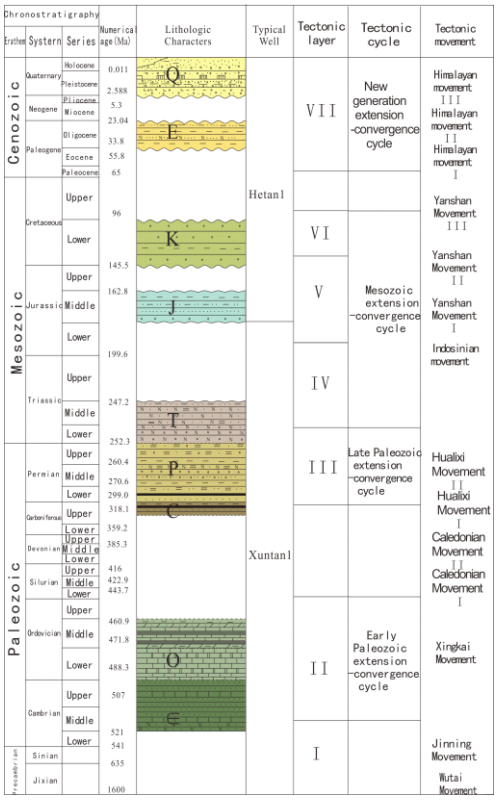

Fig.2 The comprehensive stratigraphic column of study area

2.3. Formation and Evolution of the Southern Margin of the Basin

During the Paleoproterozoic period, the evolution of global geotectonics was closely related to the aggregation and disintegration of the Columbia supercontinent and the Rodinia supercontinent. At about 2.1-1.5 Ga, the collision and aggregation of various continental blocks on the earth formed the Colombian supercontinent, and the North China Craton was generally considered to be a part of the Colombian supercontinent [5]. During the Neoproterozoic period, the Kuanping Ocean Basin was closed and the Shangdan Ocean Basin expanded on the southern margin of the North China Craton. At about 1000 Ma, Kuanping Ocean began to subduct southward. At about 900 Ma, the Kuanping Ocean closed, and the North Qinling block collided with the southern margin of the North China Craton. At about 600 Ma, the Shangdan Ocean stretched between the North Qinling block and the South China plate, and converted to a northward subduction at around 542 Ma [6]. During the Chang Cheng-Jixian period, multiple rift troughs developed in the southern part of the basin, and the basin as a whole was in an extensional environment. The whole Cambrian basin was in the stage of craton depression, and the southern margin of North China was a passive continental margin. With transgression and regression, the Cambrian in the southern part of the basin was a set of marine carbonate rocks dominated by limestone and dolomite. In the end of Early Ordovician, affected by the Huaiyuan Movement, the southern part of the basin only accepted the deposition of the Liangjiashan-Yeli Formation in some areas, and the remaining parts were lack of deposition. In the middle and late Ordovician, the basin began to accept sedimentation, forming a marine sedimentary area based on a vast land surface sea. The Caledonian movement at the end of the Early Ordovician made the entire basin uplifted and eroded, so most of the southern margin of the basin lacked the deposition of the Pingliang Formation. After that, the southern part of the basin entered a 100 million-year weathering denudation and sedimentary discontinuity. The Silurian, Devonian and Lower Carboniferous sediments were missing. The Late Carboniferous and

ISSN: 2664-9640

Permian basins were in the late period of the intracraton depression. The sedimentary system was dominated by transitional facies from land to sea, and sedimentation and subsidence were relatively stable. The Triassic inherited the sedimentary pattern of the Permian, and was dominated by continental marginal clastic deposits. In the Early and Middle Jurassic, the southern part of the basin was in a weak extension stage, and the Lower Jurassic Fuxian Formation only developed in a local area. The sediments in the southern part of the Middle-Late Jurassic basin were relatively stable, and the Anding Formation and Zhiluo Formation were mainly alluvial fan facies and lakeside-delta systems [7]. In the Late Jurassic, affected by the Yanshan Movement, the southern part of the basin uplifted as a whole, and the Anding Formation to Zhiluo Formation suffered different degrees of denudation. At the end of the Early Cretaceous, affected by the long-range effect of the closure of the Paleo-Pacific, the southern margin of the basin was strongly eroded, and the Jurassic to the Cretaceous in the middle of the southern margin were all denuded, and some stratums remained in the west. The southern part of the Cenozoic basin entered the stage of peripheral fault depression, and the Weihe graben was formed.

3. Selection of main methods and parameters

3.1. Calculation of erosion thickness

The calculation of denudation thickness is one of the important components in the study of subsidence history, and the accurate calculation of denudation thickness restricts the accuracy of basin subsidence history research. The calculation of denudation thickness mainly includes the mudstone compaction trend extrapolation method, stratigraphic correlation method, geothermal index method, and deposition rate method [8-14]. Among them, the acoustic time difference extrapolation and the geothermal index are only applicable to the thickness of the eroded stratum which was thicker than the thickness of the stratum deposited after the denudation. It is not applicable to the stratum with a smaller denudation thickness or an earlier denudation event. The stratigraphic comparison method and the deposition rate method can be applied to the strata under the above-mentioned conditions. In view the actual situation of Well Xuntan 1 in the southern part of the basin, the mudstone acoustic time difference extrapolation for the denudation thickness was used at the end of the Early Cretaceous, and the stratigraphic comparison was used for the two denudation thicknesses at the end of the Middle Triassic and the end of the Middle Jurassic. Through the mudstone acoustic time difference extrapolation method (Fig.3), the denudation thickness of Well Tentan 1 at the end of the Early Cretaceous was calculated to be 1350m. The denudation thickness at the end of the Middle Triassic was determined to be 250m and the thickness of the end of the Middle Jurassic were determined to be 100m by the stratigraphic correlation method.

3.2. Determination of ancient water depth

The restoration of water depth is a very important part of the study of the burial history of the basement of the basin. The methods of ancient water depth restoration can be divided into three main methods : sedimentology, geochemistry and paleontology [15]. This study combined the results of Tian Gang and Jiang Zaixing to qualitatively determine the ancient water depths of the basin during each period of sedimentation through sedimentary facies (Table 1) [16-17]

ISSN: 2664-9640

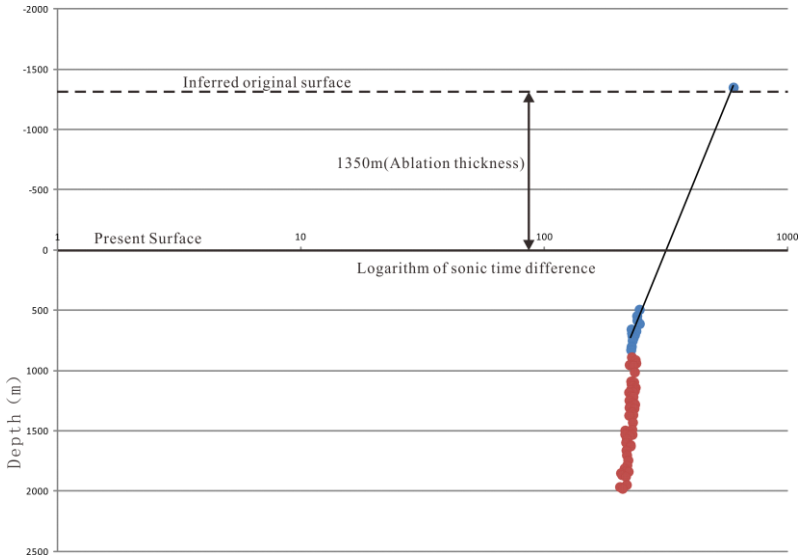

Fig.3 Calculation of erosion thickness by extrapolation of acoustic time difference of Well Xuntan-1

3.3. Restoration of burial history by back stripping method

The backstripping method is one of the main methods to restore the burial history of the basement. Its principle is to remove each set of sedimentary strata layer by layer, and restore the initial deposition thickness of the formation through the relationship curve of porosity with depth.

Before the study of burial history with the backstripping method, the relationship between porosity and depth of different lithology at single point must be analyzed. In this study, the measured porosity of sandstone and mudstone in Well Xuntan 1 and the theoretical porosity calculated by the acoustic time difference curve were calculated. Combined with the research results of denudation thickness, the relation curve between porosity and depth of sandstone and mudstone was produced (Fig.4). The limestone and dolomite were deeply buried and the rock cementation degree was high, and the porosity data can not be fitted. Therefore, the empirical parameters [3-5] are used to finally determine the limestone and dolomite. After that, the average porosity and average density of each set were calculated based on the statistics of the sandstone, mudstone, limestone, and dolomite content of each set(Table 1).

This time, the strata from the Late Triassic Yanchang Formation to the present in the study area were divided into 17 sections, the ages of the top and bottom interfaces of each section were investigated respectively, and the average density of each section was obtained (Table 1) [18-19].

On the premise of determining the above parameters, combined with the decompaction correction model, the basement burial history curve can be calculated(Fig.5).

Table.1 Table of main parameters for structural subsidence history calculation of Well Xuntan1

	Top (km)	Bot (km)	THICKNESS (km)	Sandstone (km)	mudstone (km)	limestone (km)	dolomite (km)	Avarage density (g/cm3)	average porosity	Ages of the top (Ma)	Ages of the bottom (Ma)
Chang 4+5+6	0.025	0.215	0.19	0.0949	0.0951	0	0	2.217	0.278	227	237
Chang7	0.215	0.31	0.095	0.0144	0.0806	0	0	2.261	0.262	237	241
Chang 8+9+10	0.31	1.4181	1.108	0.4452	0.6628	0	0	2.343	0.206	241	242
Zifang Formation	1.4181	1.7305	0.3124	0.0806	0.2318	0	0	2.438	0.155	242	247.2

ISSN: 2664-9640

Heshanggou Formation	1.7305	1.8624	0.1319	0.0592	0.0727	0	0	2.449	0.142	247.2	251.2
Liujiagou Formation	1.8624	2.2159	0.3535	0.1814	0.1721	0	0	2.467	0.129	251.2	252.2
Shiqianfang Formation	2.2159	2.5171	0.3012	0.1096	0.1916	0	0	2.503	0.113	252.2	260
Shihezi Formation	2.5171	2.6544	0.1373	0.0515	0.0858	0	0	2.518	0.104	260	272.3
Shanxi Formation	2.6544	2.6705	0.0161	0.0107	0.0054	0	0	2.505	0.1	272.3	290.1
Taiyuan Formation	2.6705	2.6914	0.0209	0	0.0198	0	0	2.42	0.1	290.1	298.9
Pingliang Formation	2.6914	3.0677	0.3763	0	0.0013	0.3521	0.0229	2.558	0.092	453	458.4
Majiagou Formation	3.0677	3.276	0.2083	0	0	0.0364	0.1719	2.646	0.082	458.4	470.7
Liangjiashan-Yeli Formation	3.276	3.8503	0.5743	0	0.03005	0.2169	0.3273	2.643	0.07	470.7	485.4
Sanshan Formation	3.8503	4.0077	0.1574	0	0.0067	0.0177	0.133	2.686	0.061	485.4	497
Zhangxia Formation	4.0077	4.1768	0.1691	0	0	0.0324	0.1367	2.689	0.057	497	501
Xvzhuang Formation	4.1768	4.2839	0.1071	0.0088	0.0407	0.0576	0	2.617	0.054	501	505
Maozhuang Formation	4.2839	4.323	0.0391	0.0027	0	0.0364	0	2.617	0.052	505	509

Period	Main facies	Water Depth (m)		Main Lithology	Initial porosity	Compaction factor
K-T	Inland lake facies	0-25		Sandstone	43.7	0.773
P-C	Coastal plain	25-30		Mudstone	43.4	0.372
O-∈	Shallow sea platform	30-50		limestone	36.94	0.672
				dolomite	42	0.59

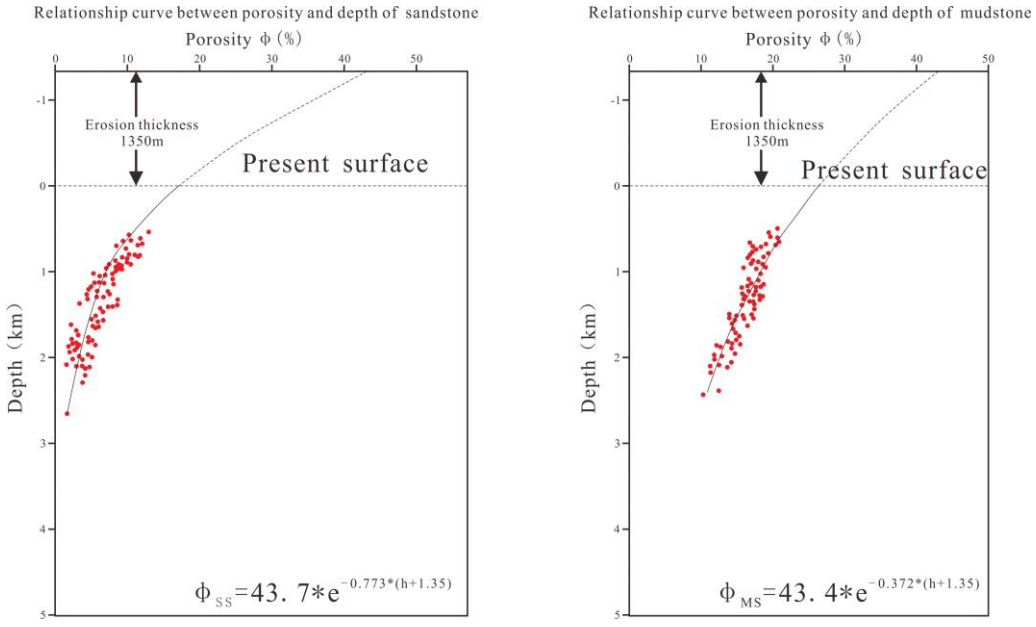

Fig.4 Relation curve between porosity and depth of sandstone and mudstone of Well Xuntan1

ISSN: 2664-9640

3.4. Calculation of structural subsindence

The tectonic subsidence of the basin is mainly calculated by removing the influence of sedimentary material load from the subsidence of the basement . According to the Airy equilibrium principle, the formula for calculating the sediment load is as follows:

$$Y_s = \mathrm{S} * \frac{\overline{\rho_s} - \rho_w}{\rho_{ma} - \rho_w}$$

In the formula,Ys is the tectonic subsidence，S is the basement subsidence，$\overline{\rho_s}$ is the average sediment density，ρ_w is the formation water density which is 1.0 g/cm^3，ρ_{ma} is the mantle density which is 3.3 g/cm^3。

The basement burial history can be calculated by calculating the relationship between the denudation thickness and porosity of a single point and the change of porosity with depth, plus the influence of ancient water depth on sedimentary material, and then removing the influence of sedimentary material load according to the Airy equilibrium model to accurately , the structural subsidence curve of Well Xuntan 1 was calculated (Fig.5).

3.5. Selection of main parameters for forward simulation

The subsidence mechanism of sedimentary basins mainly has 8 factors[20], among which the thinning of the crust, the thermal cooling of the lower crust and upper mantle, the tectonic loading of the crust and the lithosphere could be realized by numerical simulations [21-27]. In the process of applying the instantaneous tension model and post-cracking thermal depression model proposed by McKenzie and the foreland basin deflection model proposed by Allen (2013), the thickness of the lithosphere, the thickness of the upper crust of the lithosphere, and the effective elastic thickness of the lithosphere were the main factor restricting the simulation accuracy. By summarizing the research results of the predecessors on the Ordos Basin, it was believed that the crustal thickness in the southern part of the basin was 40km[30], the thickness of the lithosphere was 120km[30], and the effective elastic thickness of the lithosphere is 30km[31]. The remaining simulation parameters were constants(Table 2).

Tabel.2 Main parameters used in numerical simulation

Simulation parameters	Numerical value	Unit
Original crustal thickness	40	km
Effective elastic thickness of lithosphere	30	km
Initial lithosphere thickness	120	km
k(hermal diffusion coefficient)	0.00804	cm^2/s
τ（Thermal time constant of lithosphere）	56	Ma
Thermal expansion coefficient of lithosphere	3.28*10^{-5}	"-C"

4. Result and Discussion

4.1. Structural subsidence curve characteristics of Xuntan 1 well

The deposition period of Zhangxia, Xuzhuang, and Maozhuang formations in Well Xuntan 1 was the accelerated subsidence periods, and the subsidence rates were 44.6-52.6 m/Ma. After that, the curve entered a slow subsidence period. The subsidence rate during the deposition period of the Fengshan-Gushan Formation was 10.55 m/Ma, the subsidence rate during the deposition period of the Liangjiashan-Yeli Formation was 17.7 m/Ma, and the subsidence rate of the subsidence structure during the deposition period of the Majiagou Formation was 2.6 m/Ma. The tectonic subsidence rate during the deposition of Pingliang Formation was 16.48 m/Ma.

ISSN: 2664-9640

Due to the uplift and the denudation of the Late Caledonian period, the Silurian, Devonian and Lower Carboniferous deposits were missing in Ordos basin. The Upper Carboniferous was not developed in the periphery of Well Xuntan 1. The tectonic subsidence during the deposition period of the Permian Shanxi Formation, Taiyuan Formation, and Shihezi Formation was relatively stable with a rate of 0.5-7.8 m/Ma, which was a slow subsidence period. During the sedimentary period of the Permian Shiqianfeng Formation, Triassic Liujiagou Formation and Heshanggou Formation, the sedimentation rate had a tendency to increase, rising to 15 m/Ma, and entered an accelerated sedimentation period. During the deposition period of the Zhifang Formation, the tectonic subsidence was relatively slow, and the subsidence rate was 6.5 m/Ma. The deposition period of the 7th to 10th members of the Yanchang Formation was still an accelerated subsidence period, with a tectonic subsidence rate of 19 m/Ma. The sedimentary period of the 6th member of the Yanchang Formation to the 4th member of the Yanchang Formation was a slow subsidence period, and the tectonic subsidence rate was 0.13-5.3 m/Ma. The Middle Jurassic sedimentary period was in a slow subsidence period, and the subsidence rate was about 3 m/Ma. The Late Cretaceous was a period of accelerated subsidence, and the subsidence rate was faster than that of the Middle Jurassic, about 9 m/Ma. Later, affected by the Yanshan Movement and the Himalayan Movement, the formation above the fourth member of the Yanshan Formation were all denuded (Fig.5).

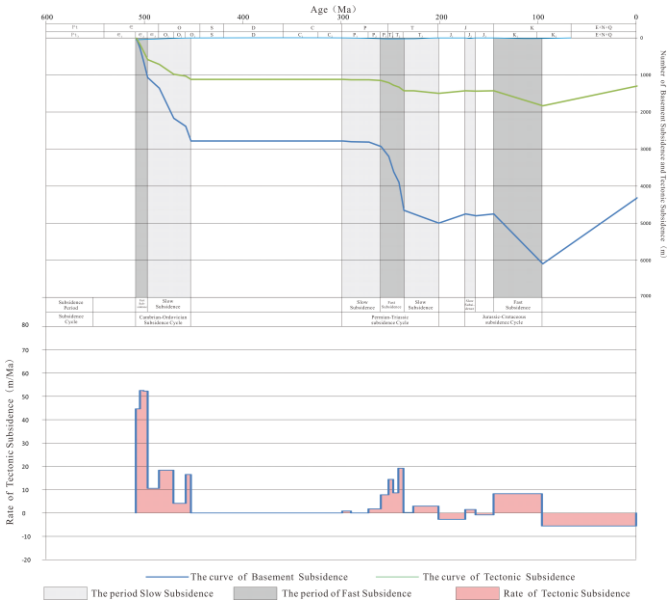

Fig.5 The subsidence's characteristic curve of Well Xuntan1

4.2. Structural subsidence stage of Xuntan 1

Based on the analysis of the tectonic subsidence curve, combined with the development characteristics of the unconformity, the tectonic subsidence in the southern part of the basin was divided into three cycles (Fig.5).

1)Cambrian-Ordovician Subsidence Cycle

This subsidence in the southern part of the subsidence cycle basin consisted of a period of rapid subsidence and a period of slow subsidence. The curve presented a concave characteristic, and the subsidence had the characteristics of rapid first and then slow. During the depositional period of the Lower Paleozoic, the Ordos Basin was in the passive continental margin stage, and was in a north-south extensional environment as a whole. The stratum subsidence was relatively stable. During the deposition period of the Zhangxia, Xuzhuang and Maozhuang formations, the basin suffered from multiple cycles of sea transgressions and recedes , and the tectonic subsidence was the fastest. In the Late Ordovician, the southern Qinling Ocean began

ISSN: 2664-9640

to subduct and the tectonic environment reversed, transforming from an extensional environment to a compressional environment, and the Upper Ordovician deposits were missing.

2)Permian-Triassic subsidence Cycle

This subsidence cycle consisted of one accelerated subsidence period and two slow subsidence periods. In the Early Permian and Middle Permian, the southern part of the basin was in the stage of land-sea alternation, and the overall settlement was relatively stable. The tectonic subsidence rate showed a trend of gradual increase, but the increasing rate was low, which was in line with the late characteristics of the settlement curve formed by the thermal cooling of deep mantle. From Late Permian to Early-Middle Triassic, the volcanic movement occurred frequently in the basin and its periphery, and the geothermal gradient in the south of the basin became higher. After the instantaneous volcanic activity, the basin began to enter the thermal cooling subsidence. Affected by this, the south of the basin entered the subsidence acceleration period. The sedimentation rate began to slow down in the Late Triassic, and the thermal cooling sedimentation entered the slow subsidence stage.

3)Jurassic-Cretaceous subsidence Cycle

The subsidence cycle consisted of a slow subsidence period and an accelerated subsidence period. During the Middle Jurassic sedimentary period, the southern basin subsidence was slow and the rate was low. In the late Early Cretaceous, affected by Qinling intracontinental orogeny and the remote response of Western Pacific subduction, the southern part of the basin entered the accelerated subsidence period

4.3. Causes of structural subsidence in Xuntan 1 well

From the perspective of the evolution process in the southern part of the Ordos Basin, during the deposition period of the Great Wall System and the Jixian System in the south of the basin, the basin was in an extensional environment and large-scale rift t . While the southern part of the basin was in a passive continent marginal stage during the deposition period of the Cambrian and Middle and Lower Ordovician[28]. From the Late Ordovician to the Carboniferous, affected by the Caledonian movement, the basin lacked sedimentation. The southern part of the Permian and Triassic basins were in the stage of intracraton depression. At the same time, a large number of volcanic clastics formed by volcanic eruptions during the same depositional period were developed in the Permian system[33,34], and tuffs were developed in the Chang 7 member, which proved that volcanic activity occurred frequently in the periphery of the Permian and Triassic basins.The thermal disturbance caused by the volcanicity changed the thermal regime and the geothermal gradient . The southern basin during Jurassic and Cretaceous periods were mainly affected by the Qinling intracontinental orogeny.

According to the analysis of the structural subsidence characteristics of Well Xuntan 1, it could be seen that the basin has mainly experienced three stages of accelerated subsidence since the Late Paleozoic. The first stage of accelerated subsidence was the deposition period of the Middle Cambrian Zhangxia, Xuzhuang and Maozhuang formations, the second stage of accelerated subsidence was the end of the Permian to the extension of the Triassic, and the third stage was the deposition of the Lower Cretaceous. .

During the first stage of accelerated subsidence, the southern part of the North China Craton was in the passive continental margin stage. The Cambrian and Ordovician were deposited on the basis of large-scale rifts in the Great Wall and Jixian periods. Therefore, the post-cracking thermal depression model was adopted to simulate the Cambrian and Ordovician tectonic subsidence curves.

When the extension factor β is 1.04692, it could be seen from the comparison of the first-stage thermal subsidence curve and the structural subsidence inversion curve that the two curves had a better fitting effect during the deposition period of the Ordovician and Cambrian strata

ISSN: 2664-9640

(Fig.6). As the entire North China Craton was uplifted and eroded by the Caledonian movement from the end of the Late Ordovician to the Early Carboniferous, and lack of deposits, regional uplift occurred from the Late Ordovician to the Late Carboniferous, and the amount of uplift and erosion on the curve was equal to the increment of the basement's tectonic subsidence. Similarly, when the Mesozoic formation was uplifted and denuded, the simulation curve must be uplifted and denuded.

The second period of accelerated subsidence was from the Late Permian to the Middle Triassic. At this time, tuff appeared in the southern part of the basin, and volcanic activities around the basin were more intense. The preliminary interpretation of the curve was that due to the transformation of the lithospheric thermal regime, thermal cooling subsidence occured after the geothermal gradient had been larger. Among them, the settlement rate in the initial stage of thermal cooling sedimentation was higher, which was an accelerated sedimentation period, and the later sedimentation was relatively stable, which was a slow sedimentation period. From the heat sink curve of the first phase simulation, it could be seen that the heat sink basically stopped at about 350 Ma. It was considered that the lithospheric geothermal gradient returned to the original value, and the thickness was returned to 120 km. Therefore, the second phase was in progress. In the simulation of the sub-thermal cooling subsidence, the parameters shown in Table 2 were still used. When the extension factor β is 1.0531, the second-stage thermal cooling subsidence curve and the structural subsidence curve obtained from the inversion had a good fitting effect from the Late Permian to the Middle Triassic (Fig.6).

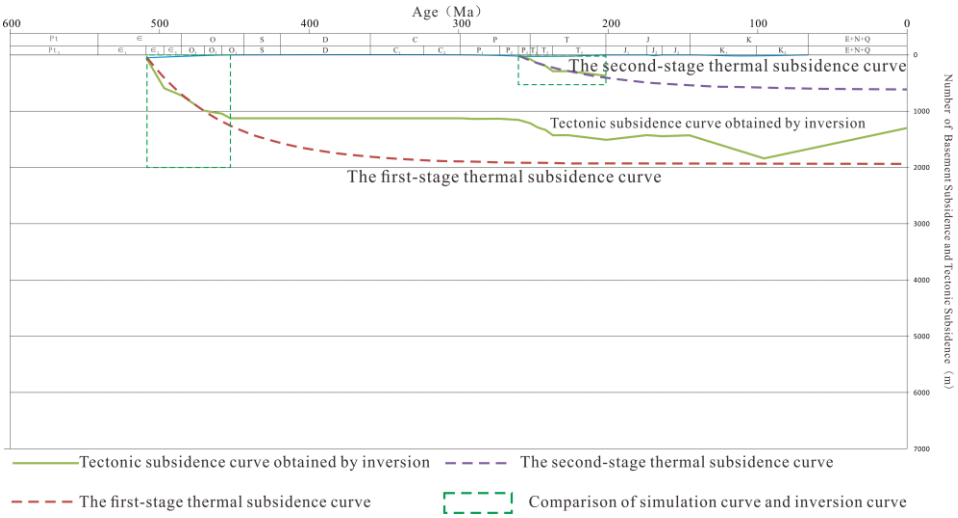

Fig.6 The staged simulation curve of Well Xuntan1

The third stage of accelerated subsidence was the Early Cretaceous. In the Early Cretaceous, the southern margin of the basin was affected by the long-range effect of the collision and closure of the Western Pacific. During this period, the Qinling Mountains was in the intracontinental orogenic stage, making the southern margin of the basin in the sedimentary environment of the intracontinental foreland basin. The structural subsidence should be the combined effect of basin thermal cooling subsidence and foreland deflection subsidence.

The study area from the Late Jurassic to the Early Cretaceous was affected by the Qinling intracontinental orogeny in the southern margin of the basin, and a giant arc-shaped nappe was superimposed on the Danfeng suture zone on the southern margin of the Qinling[32]. At this time, the foreland loading should develop on the Danfeng suture belt. Therefore, the foreland deflection model was used to simulate the cause of formation sedimentation. The Danfeng suture zone was 120km vertically from Well Xuntan 1 (Fig.1b), and the deflection simulation of the foreland basin of Well Xuntan 1 in the Early Cretaceous was carried out. (Fig.7). When the effective elastic thickness was set to 30km, according to the elastic plate model, when a load with a maximum deflection of 1156m was applied to the Danfeng suture zone, the amount of

ISSN: 2664-9640

structural subsidence caused by foreland deflection in Well Xuntan 1 during the Early Cretaceous was 826m.

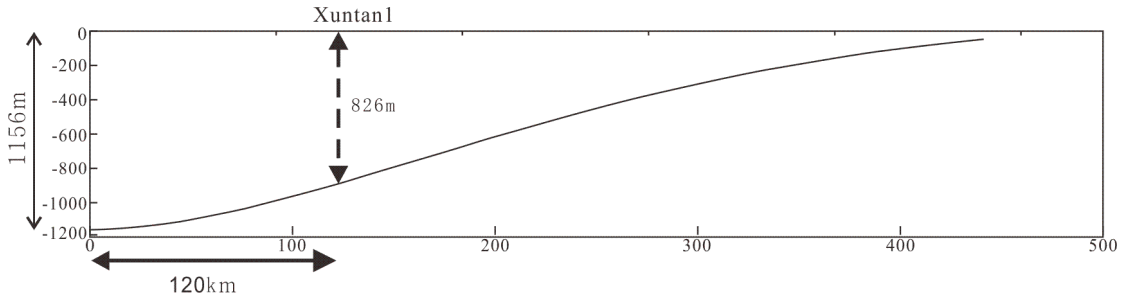

Fig.7 Simulation of foreland flexure in Early Cretaceous of Well Xuntan1

Finally, the two-stage thermal subsidence curves were combined with the simulation results of foreland deflection to produce the tectonic subsidence simulation curve under the combined action of multiple factors in Well Xuntan 1. Compared with the actual curve of tectonic subsidence curve, it could be seen that with the premise of removing uplift and erosion factors, the simulated tectonic subsidence curve was in good agreement with the actual tectonic subsidence curve (Fig.8).

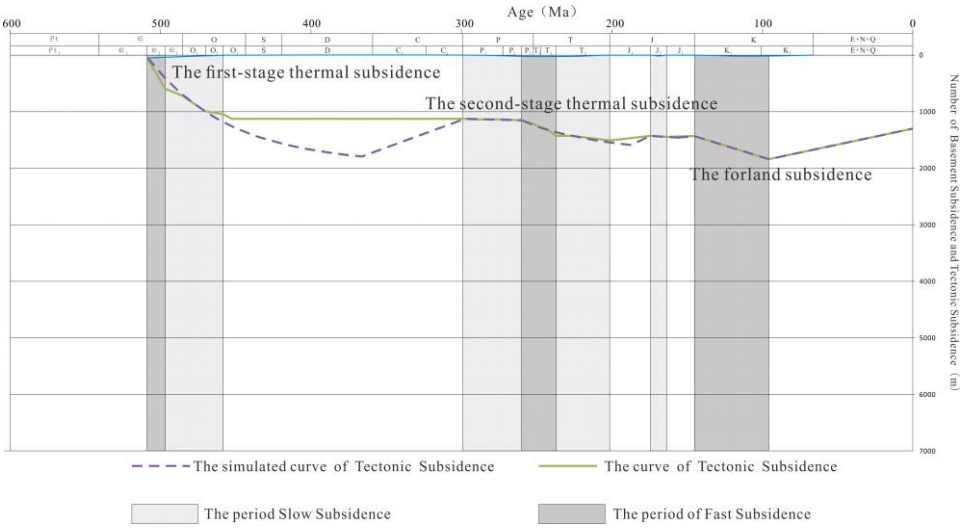

Fig.8 Comparison between actual curve and simulation curve of Well Xuntan1

5. Conclusion

(1) In the process of subsidence, the southern margin of the basin mainly experienced three rapid subsidence and two slow subsidence. The Middle Cambrian was the first accelerated subsidence period, and the subsidence rate was 44.6-52.6 m / Ma. The extension period from Late Permian to Middle Triassic was the second accelerated subsidence period, and the subsidence rate was 15-19 m / Ma. Early Cretaceous was the third accelerated subsidence period, and the tectonic subsidence rate was 9 m / Ma. Based on the characteristics of subsidence curve, the southern basin subsidence stage was divided into three stages : Cambrian-Ordovician subsidence stage, Permian-Triassic subsidence stage and Jurassic-Cretaceous subsidence stage.

(2) Based on the surrounding tectonic background, the numerical forward simulation of the structural settlement curve of Xuntan 1 well is carried out. It is considered that the first stage of accelerated settlement was due to the rapid settlement caused by the early thermal cooling settlement. The lithospheric extension factor was 1.04692, and then entered the slow settlement period. From Late Permian to Middle Triassic, the southern part of the basin was affected by volcanism and the geothermal gradient changed. The rapid subsidence in this period

ISSN: 2664-9640

was also caused by the rapid subsidence rate in the early stage of thermal cooling subsidence, and the lithospheric extension factor was 1.0531. From late Jurassic to early Cretaceous, the southern part of the basin was affected by the giant arc nappe superimposed on the Danfeng suture zone. When the load with the maximum deflection of 1156 m was applied on the Danfeng suture zone, 826 m of deflection settlement occurred in the early Cretaceous of Well Xuntan 1, and the settlement mechanism was the composite settlement caused by the deflection settlement and the thermal depression settlement.

References

[1] D.F He, G. Yang, S.W. Guan, et al. Principles and methodology of structural modeling in foreland basins, Petroleum Exploration & Development, Vol. 32 (2005) No.3, p.7-14.

[2] X.H. Liu. Basin anaylses and simulation of up-Paleozoic in Ordos basin(MS., Shanxi, Northwest University, China 2008), p.20.

[3] Z.W. Wang, G. Chen: Analysis on Mesozoic subsidence history of northeast Yishan slope of Ordos basin, Petroleum Geology and Engineering, Vol. 20 (2009) No.3, p.5+9-13.

[4] J.L. Liu, K.Y. Liu, X. Huang: Tectonic subsidence reconstruction and sedimentary responses of the Permian Shanxi and Lower Shihezi Formation in central Ordos Basin, Sedimentary Geology and Tethyan Geology, Vol. 36 (2016) No.4, p.60-70.

[5] M. Sun , N. Chen , G. Zhao , et al. U-Pb Zircon and Sm-Nd isotopic study of the huangtuling granulite, Dabie-Sulu belt, China: Implication for the paleoproterozoic tectonic history of the yangtze craton, American Journal of Science, Vol. 308 (2008) No.4, p.469-483.

[6] J. Sun , Y. Dong: Middle-Late Triassic sedimentation in the Helanshan tectonic belt: Constrain on the tectono-sedimentary evolution of the Ordos Basin, North China, Geoscience Frontiers, Vol. 10 (2019) No.1, p.213-227.

[7] J.C. Shi: The Mesozoic-Cenozoic Structural Characteristics and Its Evolution in Southern Ordos Region(MS., Shanxi, Northwest University, China 2010), p.21.

[8] W. G. Dow: Kerogen studies and geological interpretations, Journal of Geochemical Exploration, Vol. 7 (1977) No.2, p.79-99.

[9] Magara, Kin J: Compaction and fluid migration : Practical petroleum geology (Elsevier Scientific Publishign Co, USA, 1978).

[10] N.D. Naeser , C.W. Naeser , Mcculloh T H: The Application of Fission-Track Dating to the Depositional and Thermal History of Rocks in Sedimentary Basins(Springer, USA, 1989)

[11] W. Li: Summary of reconstruction of strata denudation thickness, China offshore oil and gas, Vol. 3 (1996) , p.33-37.

[12] R.Y. Chen, X.R. Luo, Z.K. Guo, et al.Estimation of Denudation Thickness of Mesozoic Stata in the Ordos Basin and Its Geological Significance, Acta Geologica Sinia, Vol. 80 (2006) No.5, p.680-693.

[13] Y. Zhong: A Summary of Erosion Thickness in Ordos Basin, Journal of Xi'an University of Arts & Science:Natural Science Edition, Vol. 14 (2011) No.3, p.103-107.

[14] C. Li, C. Jiang: Two kinds of subsidence in bansin anaylses, China Science and Technology Information, Vol. 19 (2011) p.54-55+58.

[15] J.G. Pang, Q.H. Chen, L.W. Hou, et al. The characteristics and forming mechanism of marker bed in Yanan Formation, Ordos Basin, Journal of Northwest University(Natural Science Edition). Vol. 42 (2012) No.5, p.806-812.

[16] G. Tian, L.J. Song: Thermal evolution modeling of Mesoproterozoic source rocks in the Ordos Basin, Petroleum Geology and Experiment, Vol. 39 (2017) No.4, p.520-526.

[17] Z.X. Jiang: Sedimentology. (Petroleum Industry Press, China 2010)

[18] Z.X. He, J.H. Fu, S.L. Xi, et al. Geological features of reservoir formation of Sulige gas field, Acta Petrolei Sinica, Vol. 24 (2003) No.2, p.6-12.

ISSN: 2664-9640

[19] S.H. Deng, Y.Z. Lu, Z. Luo, et al.Subdivision and age of the Yanchang Formation and the Middle - Upper Triassic boundary in Ordos Basin, North China, Science China:Earth Sciences, Vol. 48 (2018) No.10, p.31-49.

[20] J. Cathy, Busby ,V. Raymond. Ingersoll. Tectonics of sedimentary basins .(Blackwell Science, U.K. 1995.)

[21] D . Mckenzie: Some remarks on the development of sedimentary basins, Earth & Planetary Science Letters, Vol. 40 (1978) No.1, p.25-32.

[22] G.T. Jarvis , D.P. Mckenzie: Sedimentary basin formation with finite extension rates, Earth and Planetary Science Letters, Vol. 48 (1980) No.1, p.0-52..

[23] L. Royden , C.E. Keen: Rifting process and thermal evolution of the continental margin of Eastern Canada determined from subsidence curves, Earth and Planetary Science Letters, Vol. 51 (1980) No.2, p.0-361.

[24] N.J. Kusznir , P.A. Ziegler: The mechanics of continental extension and sedimentary basin formation: A simple-shear/pure-shear flexural cantilever model, Tectonophysics, Vol. 215 (1992) No1-2, p.117-131.

[25] D.B. Rowley,D. Sahagian: Depth-dependent stretching: A different approach, Geology, Vol. 14 (1986) No1, p.32.

[26] C.S. Lin, Y.M. Zhang, S.T. Li et al. Episodic Rifting Dynamic Process and Quantitative Model of Mesozoic-Cenozoic Faulted Basins in Eastern China, Earth Science-Journal of China University of Geosciences, Vol. 29 (2004) No5, p.583-588.

[27] P.A. Allen,J.R. Allen: Basin Analysis: Principles and Application to Petroleum Play Assessment(Wiley Blackwell, USA 2013.)

[28] Z.Y. Zhao, Y.R. Guo, Y. Wang, et al. The Research progress in structural evolution and paleogeographic characteristics of Ordos Basin, Special Oil & Gas Reservoirs, Vol. 19 (2012) No5, p.19-24+155.

[29] J. Liao, D. Zhou, Z.X. Zhao: Numerical models of the tectono-thermal evolution of rift basins and their applications to the Northern South China Sea, Journal of Tropical Oceanography, Vol. 28 (2009) No6, p.43-53.

[30] B. Xia. Lithosphere structure of the North China Block(Ph.D. Wuhan China University of Geosciences (Wuhan),China 2017) p.66.

[31] B. Chen: The Effective Elastic Thickness over China and Surroundings and Its Lithosphere Dynamic Implication, (Ph.D. Beijing China University of Geosciences,China 2013), p.70.

[32] G.W. Zhang, Y.P. Dong, S.C. Lai, et al.MIANLUE structural belt and MIANLUE suture zone in the southern margin of Qinling Dabie orogenic belt, Science in China (Series D), Vol. 33 (2003) No12, p.1121-1135.

[33] H. Yang, Y.H. Yang, X.H. Shi, et al. Influence of the Late Paleozoic Volcanic Activity on the Sandstone Reservoir in the Interior of Ordos Basin, Acta Sedimentologica Sinica, Vol. 4 (2007) p.526-534.

[34] H.P. Bao, Y.H. Yang, X.F. Wang, et al. Significance of synsedimentary volcanism for formation of sandstone reservoirs of the Upper Paleozoic in Ordos Basin, Journal of Palaeogeography, Vol. 4 (2007), p.394-406.